The so-called dry laser cleaning governed by humidity at the nanometer scale

David Grojo, Ph. Delaporte, M. Sentis, O. Pakarinen, A. Foster

The so-called dry laser cleaning governed by humidity at the nanometer scale

D. Grojo,* Ph. Delaporte,† and M. Sentis
LP3, UMR 6182, CNRS - Université de la Méditerranée, Case 917, 13288 Marseille Cedex 9, France

O.H. Pakarinen and A.S. Foster
Laboratory of Physics, Helsinki University of Technology, P.O.Box 1100, FI-02015 TKK, Finland
(Dated: December 17, 2007)

Illumination with single nanosecond pulses leads to the detachment of silica particles with 250-nm radii from silicon surfaces. We identify two laser-energy dependent cleaning regimes by time-of-flight particle-scattering diagnostics. For the higher energies, the ejection of particles is produced by nanoscale ablation due to the laser field enhancement at the particle-surface interface. The damage-free regime at lower energy is shown to be governed by the residual water molecules which are inevitably trapped on the materials. We discuss the great importance that the humidity plays on the cleaning force and on the adhesion in the experiments.

Applied Physics Letters, Accepted, Dec. 2007.

PACS numbers: 42.62.-b, 68.08.-p

Pulsed laser radiation can induce the detachment of nanometer-size particles from various materials surfaces allowing a laser process to be envisioned for advanced cleaning applications related to the fabrication of nanoscale devices [1, 2]. However, although the dry laser cleaning (DLC) approach has been extensively studied for more than 15 years now, there is still a lack of knowledge of its underlying mechanisms. Studies have identified different physical processes which contribute to the cleaning force, but little is known about the importance of each of them. Historically, DLC was explained on the basis of a mechanical ejection resulting from the rapid thermal expansion of the irradiated materials [3] and described accurately by recent models [4, 5]. However, Mosbacher *et al.* [6] reported that damage free DLC is impossible with short pulses (< 6 ns). The local substrate ablation due to the optical near field enhancement underneath the particles is the dominant cleaning mechanism for all their tested situations. In addition, further experimental investigations showed a relatively strong ambient humidity dependence of the particle removal efficiency [7, 8]. They revealed that the cleaning force provided by the laser-evaporated water which is previously condensed from the ambient onto the surface materials can be of particular importance.

In this letter, we measure the laser pulse energy dependence of the time-of-flight (TOF) of the removed particles to identify (by the ejection dynamics) the validity domains of these processes. The irradiated materials are isolated 250-nm radius silica spheres (Kisker-Biotech) supported by silicon (100) substrates. The native oxide layer coverage of the surfaces makes them hydrophilic. We measured a water contact angle of 18 ± 2 degrees. The samples are placed in a vacuum chamber with a residual pressure less than 5×10^{-2} Pa to avoid slow-

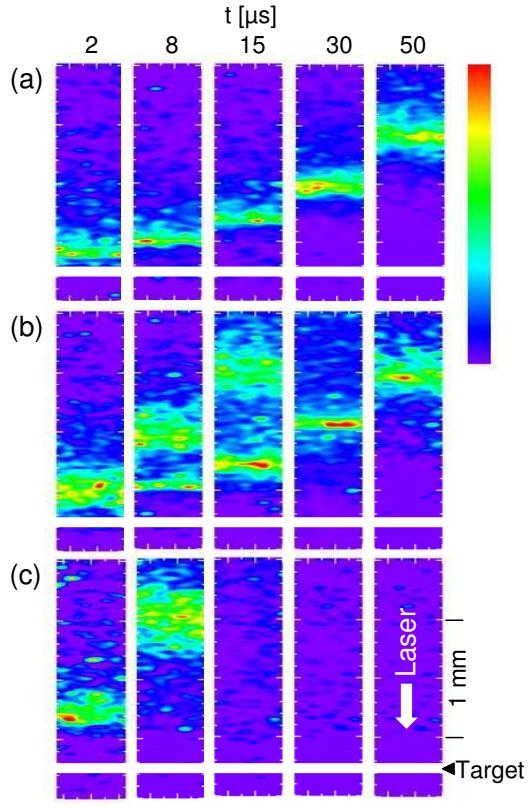

FIG. 1: (color online) Scattering images of the ejected particles for different laser fluences F_{las}: (a) $F_{las} = 275$ mJ cm^{-2}, (b) $F_{las} = 415$ mJ cm^{-2}, (c) $F_{las} = 550$ mJ cm^{-2}. The particle cloud propagation is analyzed by capturing images for different delays t between the cleaning laser pulse and the observation gate (1 μs).

*Electronic address: david.grojo@nrc-cnrc.gv.ca; Also at: National Research Council, Steacie Institute for Molecular Sciences, 100 Sussex Drive, Ottawa, Ontario K1A 0R6, Canada
†Electronic address: delaporte@lp3.univ-mrs.fr

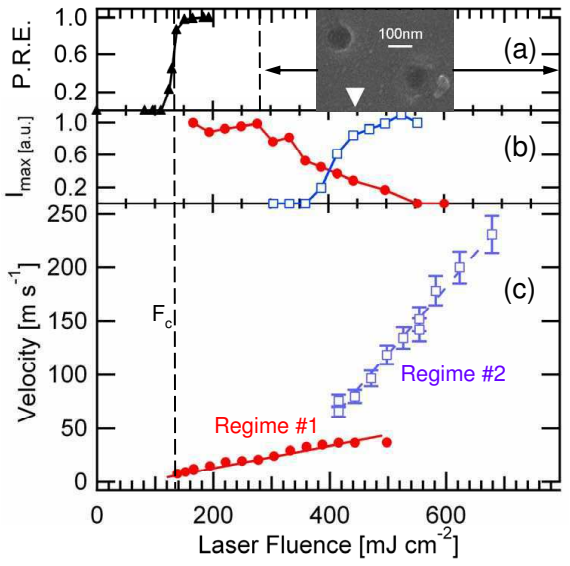

FIG. 2: (a) Particle Removal Efficiency PRE, (b) maximum scattering intensity I_{max} and (c) particle velocity corresponding to each ejected cloud as a function of the laser fluence F_{las}. The scattered intensity for the slow (resp. fast) component was measured for a time delay t set to 10 μs (resp. 20 μs). The embedded SEM image shows the ablated craters observed for $F_{las} \approx 430$ mJ cm^{-2}.

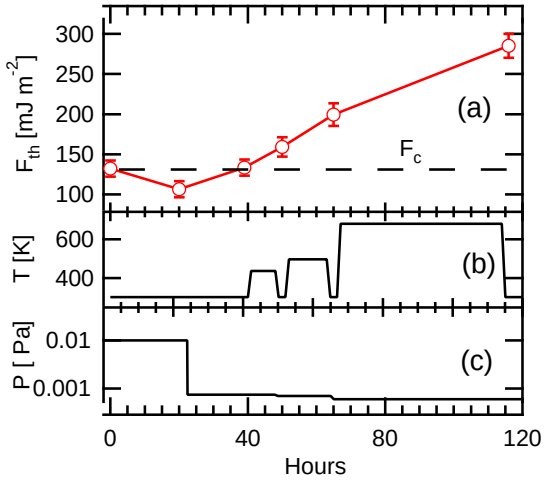

FIG. 3: Increase of the particle removal fluence threshold F_{th} over time when water vapor progressively desorbs from surfaces (a). The sample holder in the vacuum chamber is backside equipped with a halogen lamp to perform successive baking steps (b) under a decreasing atmosphere pressure (c).

ing down of the particles in the observed region. The cleaning laser was an ArF ($\lambda_{las} = 193$ nm) excimer laser source (Lambda Physik, LPX220i) delivering pulses of 15-ns duration. An experimental approach based on forward scattering detection is used to perform the TOF measurements. The experimental configuration is described in detail in ref. [9]. As the ejected particles propagate into a CW probe beam ($\lambda = 532$ nm), we perform time- and space-resolved imaging of the particle clouds with the aid of a fast intensified CCD (Princeton Instruments, model 576/RB-E).

Figure 1 shows the images captured for different laser fluences F_{las} and delays t varying from 10 to 120 μs. For $F_{las} = 415$ mJ cm^{-2}, we observe as unique feature the detachment of the particles divided into two distinct components propagating with different velocities (fig. 1b). Although we study calibrated systems, this observation is in support of the coexistence of two distinct mechanisms leading to the ejection of particles. The only presence of the slow (resp. fast) component for lower (resp. higher) fluences is in agreement with a regime where a single mechanism dominates (fig. 1a,c).

To analyze these regimes in more detail, figure 2 provides the determined detachment velocities of the particles as a function of the laser fluence. Based on optical microscopy analyses, figure 2a presents the proportion of the particles (PRE) which are removed by the irradiation as a function of the laser fuence. A sharp threshold value $F_{th} = F_c \approx 130$ mJ cm^{-2} is found, above which more than 95% of the particles are removed. Above F_c, particles are ejected with a characteristic velocity gradually increasing from 7.6 to 36.8 m s^{-1} (regime #1, fig. 2c). In the range 300–500 mJ cm^{-2}, the scattered intensity from the particle cloud decreases while a faster component signal prevails (fig. 2b). This evidences the transition between two regimes with different mechanisms. In the highest fluence regime (regime #2), the remained particle cloud acquires considerably more speed when increasing laser fluence. Propagation velocity of this scattering component linearly increases from 66 to 231 m s^{-1} when fluence is varied from 415 to 680 mJ cm^{-2}.

We carefully analyzed, by means of Scanning Electron Microscopy (SEM) and Atomic Force Microscopy (AFM), the effect of the laser pulse energy on the surfaces. In agreement with the systematic observation of ablated craters (fig.2a) for F_{las} above 280 mJ cm^{-2}, the fast ejection dynamics regime (#2) is governed by a local substrate ablation mechanism. The typical diameter of the ablated craters is 130±15 nm which is consistent with the spatial distribution of the near field enhancement calculated by the Mie theory [10]. In this fluence range, the estimated surface temperature reaches values above the evaporation temperature of silicon (2628 K). Then, the particle velocity is gained by momentum transfer from the ablated species.

The existence of the regime #1 in which we do not observe damage, shows that the removal by a damage-free process is feasible. However, its identification becomes more complex. First, the measured ejection velocity for laser fluences slightly above F_c is two orders of magnitude higher than the thermally-induced expansion velocity of the substrate for similar conditions [9, 11]. Thus, we concluded that the dynamics of materials is not fast enough to explain the detachment of particles in the experiments.

This regime exhibits ejection velocities which remain more likely compatible with another ablative mechanism. It is known that hydrophilic silicon exposed to ambient air with its attendant humidity becomes covered with, at minimum, a monolayer of water molecules. Experimental analyses reveal also spontaneous adsorption of water molecules into small interstices even in ultrahigh vacuum [12]. Thus, it is worthwhile to examine the role that the laser ablation of the trapped humidity can play in these experiments which are performed without delay after the substrates are placed in the vacuum chamber. As shown in figure 3, we heated the samples to progressively desorb water from the surfaces. Then, the laser energy threshold measurements (see fig. 2a) are repeated at ambient temperature $T_0 \cong 300$ K between each baking step (fig. 3.b) to evaluate the role of the evaporated water molecules. Figure 3 shows that the reduction of humidity over time is accompanied by an apparent increase in the laser energy required to eject the particles. For the studied situation, the removal threshold fluence changes by a factor $\cong 2.1$ (fig. 3.a) and reaches a value which is similar to the substrate damage threshold *i.e.* where only the first identified ejection mechanism plays a role. This is clear evidence that the presence of water in the studied systems is required for the existence of the ejection mechanism responsible for the regime #1.

The adhesion of dry submicrometer objects to surfaces is mainly provided by the van der Waals forces. A typical value of this adhesion force for submicron particles is $\approx$ 100 nN [13]. Nevertheless, numerous authors report the formation of a water meniscus at the nanoparticle-surface interstices for moderated relative humidity (RH) atmospheres [14, 15]. In this case, the subsequent contribution of the capillary force to the adhesion is usually estimated by the standard approximation $F_c = 4\pi\gamma R$, where γ is the surface tension of water (7.28×10^{-4} N cm^{-1}). For particles as small as $R = 250$ nm, this force ($\approx$ 220 nN) is not negligible and can clearly dominate the interaction. However, since the saturated vapor pressure of water is 2340 Pa, our pressure atmosphere of 10^{-2} Pa (in the initial stage) means $RH \cong 10^{-3}$%. For this humidity, the Kelvin equation gives a curvature radius of 0.5 Å for the condensed liquid meniscus. Thus, our system is clearly out of the validity domain of these continuum models and a real liquid meniscus cannot be envisioned. However, the figure 3 shows that the removal threshold F_{th} exhibits a non-monotonous evolution when water progressively desorbs. In a first stage (< 20 h), we measured a fluence threshold reduction to $\approx 0.8 \times F_c$ as well as a significant increase of the particle kinetic energy $\Delta E_k/E_k \cong 2.7$. According to ref.[12], this may indicate the elimination of some residual water molecules which were still trapped into the contact line of the particles and which contributed to the adhesion (at t_0). Indeed, the desorption rate of these molecules during pump-down is initially faster than that of those forming the surface monolayer coverage since water-to-water bonds are weaker than water-to-solid ones [16]. Then, particle-surface adhesion and the subsequent removal threshold decreases before than the monolayer is affected. The laser threshold measurements show that the contribution of these trapped molecules to the total particle-surface adhesion is about 20% (initially). This is a relatively strong effect for a very low water volume such as expected. In fact, assuming the 250-nm spheres are compressed according to the JKR theory predictions (10 nm radius contact area) and a maximum of ≈ 4 water molecules layer are trapped into the particle contact lines, we still have more than 100 times more molecules in the monolayer underneath the particle (10 nm to 250 nm from the center) than in the molecular meniscus. From these estimations combined with our observations, we can conclude that a molecular-size meniscus can still exist under vacuum. However, the ejection of particles results mainly from the laser ablation of the water monolayer coverage rather than that of the meniscus as it was established for studies at higher RH where real liquid meniscus are formed [7, 8].

In conclusion, our results emphasize that the presence of molecular residual water offers possibility to achieve damage-free laser nano-cleaning in a limited energy-operating window (regime #1). This is of practical importance for applications like microelectronics, where strictly non-consuming substrate cleaning methods are needed. We highlight that the humidity governs most of physical processes naturally involved in the experiments. However, since in vacuum the water molecules do not form real menisci below particles, continuum models fail. For real quantitative analysis of the role of water in the studied systems, we emphasize that molecular studies would be needed. Operation in regime #2 defines a region to produce patterning of solid surfaces with near-field resolutions. Studies on this aspect [10, 17, 18] should lead to the development of photonic-based colloidal lithography techniques for creating various functional nanostructured materials.

[1] W. Zapka, W. Ziemlich, and A. C. Tam, Appl. Phys. Let. **58**, 2217 (1991).

[2] O. Yavas, N. Suzuki, M. Takai, A. Hosono, and S. Kawabuchi, Appl. Phys. Let. **72**, 2797 (1998).

[3] A. C. Tam, W. P. Leung, W. Zapka, and W. Ziemlich, J. Appl. Phys. **71**, 3515 (1992).

[4] N. Arnold, Appl. Surf. Sci. **208**, 15 (2003).

[5] B. S. Luk'Yanchuk, Z. B. Wang, W. D. Song, and M. H. Hong, Appl. Phys. A **79**, 747 (2004).

[6] M. Mosbacher, H. J. Munzer, J. Zimmermann, J. Solis, J. Boneberg, and P. Leiderer, Appl. Phys. A **72**, 41 (2001).

[7] G. Vereecke, E. Rohr, and M. M. Heyns, J. Appl. Phys. **85**, 3837 (1999).

[8] M. Mosbacher, M. Bertsch, H. J. Munzer, V. Dobler, B. U. Runge, D. Bauerle, J. Boneberg, and P. Leiderer, Proc. SPIE **4426**, 308 (2002).
[9] D. Grojo, A. Cros, P. Delaporte, and M. Sentis, Appl. Phys. B **84**, 517 (2006).
[10] A. Pereira, D. Grojo, M. Chaker, P. Delaporte, D. Guay, and M. Sentis, Unpublished (2007).
[11] V. Dobler, R. Oltra, J. P. Boquillon, M. Mosbacher, J. Boneberg, and P. Leiderer, Appl. Phys. A **69**, S335 (1999).
[12] R. A. Nevshupa, M. Scherge, and A. S. I., Surf. Sci. **517**, 17 (2002).
[13] F. W. Delrio, M. P. De Boer, J. A. Knapp, E. D. Reedy, P. J. Clews, and M. L. Dunn, Nature Materials **4**, 629 (2005).
[14] M. Schenk, M. Futing, and R. Reichelt, J. Appl. Phys. **84**, 4880 (1998).
[15] O. H. Pakarinen, A. S. Foster, M. Paajanen, T. Kalinainen, J. Katainen, I. Makkonen, J. Lahtinen, and R. M. Nieminen, Modelling Simul. Mat. Sci. Eng. **13**, 1175 (2005).
[16] P. Danielson, R&D Mag. **43**, 57 (2001).
[17] W. J. Cai and R. Piestun, Appl. Phys. Let. **88**, 111112 (2006).
[18] Y. Zhou, M. H. Hong, J. Y. H. Fuh, L. Lu, B. S. Luk'yanchuk, Z. B. Wang, L. P. Shi, and T. C. Chong, Appl. Phys. Let. **88**, 023110 (2006).